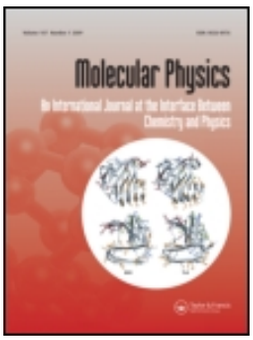

Molecular Physics

ISSN: 0026-8976 (Print) 1362-3028 (Online) Journal homepage: http://www.tandfonline.com/loi/tmph20

A variational method for the calculation of ro-vibronic levels of any orbitally degenerate (Renner-Teller) triatomic molecule

S. Carter & N.C. Handy

To cite this article: S. Carter & N.C. Handy (1984) A variational method for the calculation of ro-vibronic levels of any orbitally degenerate (Renner-Teller) triatomic molecule, Molecular Physics, 52:6, 1367-1391, DOI: 10.1080/00268978400101981

To link to this article: http://dx.doi.org/10.1080/00268978400101981

MOLECULAR PHYSICS, 1984, VOL. 52, NO. 6, 1367–1391

A variational method for the calculation of ro-vibronic levels of any orbitally degenerate (Renner–Teller) triatomic molecule

by S. CARTER
Department of Chemistry, University of Reading,
Whiteknights, Reading, England
and N. C. HANDY
University Chemical Laboratory, Lensfield Road,
Cambridge, CB2 1EW, England

(*Received* 31 *January* 1984; *accepted* 26 *March* 1984)

The variational method for the determination of ro-vibrational energy levels has been extended to the ro-vibronic energy levels of Renner–Teller triatomic molecules. A previously derived hamiltonian $\mathscr{H}(R_1, R_2, \theta, \hat{\mathbf{\Pi}})$ has been used, with $\hat{\Pi}_z$ replaced by $\hat{\Pi}_z + \hat{L}_z$. Expansion functions having the correct symmetry in $D_{\infty h}(\Sigma_g^+, \Sigma_g^-, \Sigma_u^+, \Sigma_u^-)$ or $C_{\infty v}(\Sigma^+, \Sigma^-)$ are selected, for any J value, from a recipe which is general for any type of Renner–Teller system.

The method is demonstrated for the lowest A' and A'' surfaces of CH_2^+, whose analytic representation has been obtained from *ab initio* data. The barrier to linearity is 931 cm^{-1} for the A' state. Ro-vibronic levels for $J \leqslant 2$, up to 9000 cm^{-1} above the A' minimum ($\alpha_e = 137°$) are determined. The bending levels show the same Renner–Teller characteristic interaction determined by other workers who have included the effect of the stretches in a less rigorous way. Fermi-resonance between specific energy levels does not appear to be important for the reported levels of CH_2^+, although it is shown that there are marked differences in the calculated spectra when the stretching modes are omitted.

1. INTRODUCTION

Much progress has been made in recent years on the determination of the ro-vibrational energy levels of triatomic molecules. If we assume that the potential energy surface has a given analytical form $V(R_1, R_2, \theta)$, in terms of two bond lengths R_1, R_2 and the included bond angle θ, then the problem is the determination of the ro-vibrational energy levels for this surface.

The best approach is to solve the appropriate Born–Oppenheimer equation for nuclear motion

$$(T_N + V - W)\psi_N = 0. \tag{1}$$

This may be solved by the variational method, representing ψ_N as a linear combination of expansion functions $\sum_{s=1}^{M} c_s \Phi_s$. Recently Sutcliffe and ourselves gave an explicit expression for T_N in terms of R_1, R_2, θ and $\hat{\mathbf{\Pi}}$, where $\hat{\mathbf{\Pi}}$ is the angular momentum operator [1]. This paper [1] is the latest in a series of many articles which discuss the best representations to use for T_N and for the expansion

functions Φ_s, in the variational method. The interested reader is referred to the review article by Carney, Sprandel and Kern [2] and our article [3] which gives more detail of the approach now recommended by us using the kinetic energy operator in [1].

The alternative approach which has met with great success is the use of the rigid-bender Hamiltonian originally due to Hougen, Bunker and Johns [4]. This approach leads to a derived hamiltonian $H_N(\theta)$, where the effects of the stretching motions may be included by second-order perturbation theory. Such a hamiltonian has been used for the interpretation of the bending vibrational spectra of ' floppy ' molecules [5].

In this paper, we tackle the problem where two potential energy surfaces must be treated together, namely the Renner–Teller problem. The potential surfaces, whose electronic wavefunctions are denoted $X(A'$ in $C_s)$ and $Y(A'')$, are degenerate when the molecule is linear, and the nuclear motion wavefunction is represented as

$$\Psi_N = \psi_{N_X} X + \psi_{N_Y} Y.$$

The ro-vibronic levels of the X and Y surfaces may not be treated separately when $J \neq 0$ because of the coupling of the electronic and rotational angular momenta. Here we discuss in detail the variational method for the solution of this problem, with particular application to the CH_2^+ molecule. Of course the Renner–Teller problem has been discussed by many workers, following the original work of Renner and Teller [6], which is described by Herzberg [7]. Pople and Longuet–Higgins [8] used the simplest form for $H_N(\theta)$ to interpret the experimental results obtained by Dressler and Ramsay [9] for NH_2. Since that time there have been successive improvements of this approach by Barrow, Dixon and Duxbury [10], Duxbury and Dixon [11] and Jungen and Merer [12], each of whom used the rigid-bender hamiltonian, with particular application to NH_2. These workers have as a result determined sections of both the X and Y surfaces of NH_2. More recently Buenker, Peyerimhoff and co-workers [13, 14] have used *ab initio* potential energy surfaces and properties, within the same framework, to make *ab initio* predictions for the bending ro-vibronic levels of NH_2.

In this paper we shall compare the variational method with the rigid-bender method, to see in particular if there are any aspects of this problem which unexpectedly occur with a full variational treatment of the effects of the stretching motions, and a full treatment of angular momentum. Predictions will be made for the (unobserved) ro-vibronic spectra of CH_2^+, using potential energy surfaces which are determined with the help of *ab initio* data.

2. The ro-vibronic hamiltonian and associated expansion functions

A hamiltonian $H(R_1, R_2, \theta, \hat{\Pi})$ for the ro-vibrational motion of a triatomic molecule was given in [1] as

$$H = H_V(R_1, R_2, \theta) + H_{VR}(R_1, R_2, \theta, \hat{\Pi}). \tag{3}$$

$\hat{\Pi}$ is the total angular momentum operator relative to body-fixed axes, and it depends on the Euler angles α, β, γ. This hamiltonian was derived with the general theory of Sutcliffe [15]. In that general theory, Sutcliffe included the

effects of both nuclear and electronic motion, and it follows from that theory that, if electronic motion is included, $\hat{\mathbf{\Pi}}$ should be replaced by $\hat{\mathbf{\Pi}}+\hat{\mathbf{L}}$ in H_{VR}, where $\hat{\mathbf{L}}$ is like an electronic angular momentum operator. In full, then the hamiltonian for the Renner–Teller problem is

$$\begin{aligned}H_{\mathrm{V}}(R_1, R_2, \theta) = &-\frac{\hbar^2}{4}\left(\frac{1}{\mu_1 {R_1}^2}+\frac{1}{\mu_2 {R_2}^2}-\frac{2\cos\theta}{mR_1R_2}\right)\left(\frac{\partial^2}{\partial\theta^2}+\cot\theta\,\frac{\partial}{\partial\theta}\right)\\ &-\frac{\hbar^2}{2\mu_1}\frac{\partial^2}{\partial {R_1}^2}-\frac{\hbar^2}{2\mu_2}\frac{\partial^2}{\partial {R_2}^2}-\frac{\hbar^2}{4}\left(\frac{\partial^2}{\partial\theta^2}+\cot\theta\,\frac{\partial}{\partial\theta}\right)\\ &\times\left(\frac{1}{\mu_1 {R_1}^2}+\frac{1}{\mu_2 {R_2}^2}-\frac{2\cos\theta}{mR_1R_2}\right)-\frac{\hbar^2\cos\theta}{m}\frac{\partial^2}{\partial R_1\,\partial R_2}\\ &+\frac{\hbar^2}{m}\left(\frac{1}{R_1}\frac{\partial}{\partial R_2}+\frac{1}{R_2}\frac{\partial}{\partial R_1}\right)\left(\sin\theta\,\frac{\partial}{\partial\theta}+\cos\theta\right)+V,\end{aligned}$$

and

$$\begin{aligned}&H_{\mathrm{VR}}(R_1, R_2, \theta, \hat{\mathbf{\Pi}}, \hat{\mathbf{L}})\\ &=\frac{1}{8\cos^2\theta/2}\left(\frac{1}{\mu_1 {R_1}^2}+\frac{1}{\mu_2 {R_2}^2}+\frac{2}{mR_1R_2}\right)(\hat{\Pi}_z+\hat{L}_z)^2\\ &\quad+\frac{1}{8\sin^2\theta/2}\left(\frac{1}{\mu_1 {R_1}^2}+\frac{1}{\mu_2 {R_2}^2}-\frac{2}{mR_1R_2}\right)(\hat{\Pi}_x+\hat{L}_x)^2\\ &\quad+\tfrac{1}{8}\left(\frac{1}{\mu_1 {R_1}^2}+\frac{1}{\mu_2 {R_2}^2}+\frac{2\cos\theta}{mR_1R_2}\right)(\hat{\Pi}_y+\hat{L}_y)^2\\ &\quad-\frac{1}{4\sin\theta}\left(\frac{1}{\mu_1 {R_1}^2}-\frac{1}{\mu_2 {R_2}^2}\right)((\hat{\Pi}_z+\hat{L}_z)(\hat{\Pi}_x+\hat{L}_x)+(\hat{\Pi}_x+\hat{L}_x)(\hat{\Pi}_z+\hat{L}_z))\\ &\quad+\frac{\hbar}{2i}\left[\left(\frac{1}{\mu_1 {R_1}^2}-\frac{1}{\mu_2 {R_2}^2}\right)\left(\frac{\cot\theta}{2}+\frac{\partial}{\partial\theta}\right)\right.\\ &\qquad\left.+\frac{\sin\theta}{m}\left(\frac{1}{R_2}\frac{\partial}{\partial R_1}-\frac{1}{R_1}\frac{\partial}{\partial R_2}\right)\right](\hat{\Pi}_y+\hat{L}_y). \qquad (4)\end{aligned}$$

The particular choice of body fixed axes has the molecule lying in the zx plane, with Ox bisecting the angle θ. m is the mass of the central atom, situated at O, and μ_1, μ_2 are reduced masses.

The expansion functions for the variational problem are written as a product of well-chosen vibrational, electronic and rotational functions. We choose the following expansion functions for the bending, electronic and rotational motion, labelled $\Psi_{V_3}^{J,k,\lambda}(\theta, \beta, \gamma, \mathbf{r})$

$$\Psi_{V_3}^{J,k,\lambda}(\theta, \beta, \gamma, \mathbf{r}) = P_{n_3}^{|k-\lambda|}(\cos\theta)D_{0k}^{J}(\beta, \gamma)\Phi_{\mathrm{e}}^{\lambda}(r). \qquad (5)$$

$P_{n_3}^{|l|}$ are associated Legendre polynomials of degree $n_3 = 2V_3 - |l|$, and $|l| = |k-\lambda|$. $\Phi_{\mathrm{e}}^{\lambda}(\mathbf{r})$ are the appropriate combinations $X \pm iY$ of the electronic wavefunctions of the two surfaces ($\lambda = \pm 1$). When the molecule has $D_{\infty h}$ symmetry, $\Phi_{\mathrm{e}}^{\lambda}(\mathbf{r})$ are eigenfunctions of $\hat{L}_z = -i\hbar(\partial/\partial\phi)$ with eigenvalues $\lambda\hbar$. $D_{0k}^{J}(\beta, \gamma)$ are the $M=0$ (and therefore independent of α) rotational wavefunctions introduced in

previous work [3], which obey $\hat{\Pi}_z D_{0k}^J = -k\hbar D_{0k}^J$. (Recall that $\hat{\boldsymbol{\Pi}}$ is the angular momentum operator with respect to body-fixed axes, with

$$[\hat{\Pi}_x, \hat{\Pi}_y] = i\hbar\hat{\Pi}_z \quad \text{and} \quad \hat{\Pi}_z = i\hbar(\partial/\partial\gamma)).$$

γ denotes the orientation of the body fixed axis with respect to the space fixed axis, and ϕ denotes the orientation of the odd electron with respect to the body fixed axis.

The hamiltonian $H_V + H_{VR}$ is singular when the molecule is linear ($\theta = \pi$), due to the presence of terms $\hat{A}$, where

$$\hat{A} = -\frac{\hbar^2}{2}\left(\frac{1}{\mu_1 R_1^2} + \frac{1}{\mu_2 R_2^2} - \frac{2\cos\theta}{mR_1R_2}\right)\left(\frac{\partial^2}{\partial\theta^2} + \cot\theta\frac{\partial}{\partial\theta}\right) + \frac{1}{8\cos^2\theta/2}\left(\frac{1}{\mu_1 R_1^2} + \frac{1}{\mu_2 R_2^2} + \frac{2}{mR_1R_2}\right)(\hat{\Pi}_z + \hat{L}_z)^2. \quad (6)$$

The principal reason for choosing the form of $\Psi_{V_3}^{J,k,\lambda}$ in (4) is that it may easily be shown that $\hat{A}\Psi_{V_3}^{J,k,\lambda}$ is not singular at $\theta = \pi$ because of the cancellation of the $\sin^{-2}\theta$ terms arising from

$$\left(\frac{\partial^2}{\partial\theta^2} + \cot\theta\frac{\partial}{\partial\theta}\right)P_n^l(\cos\theta) \equiv -\left(n(n+1) - \frac{l^2}{\sin^2\theta}\right)P_n^l(\cos\theta),$$

with the $\cos^{-2}(\theta/2)$ terms.

The symmetry properties of a ro-vibronic eigenfunction are labelled by $+$ or $-$, depending on whether the function is changed on inversion. It is labelled g or u depending on whether it is changed or unchanged upon exchange of the identical nuclei. Following Bunker and Papousek [16] the eigenfunctions may therefore be labelled Σ_g^+, Σ_g^-, Σ_u^+, Σ_u^-. We now discuss the possible symmetries of $\Psi_{V_3}^{J,k,\lambda}$ using $D_{\infty h}$ labels, following the ideas of [16], which will lead to the appropriate combination of our expansion functions which have the above symmetries.

At linear geometries, we may write

$$\Psi_{V_3}^{J,k,\lambda}(\theta, \beta, \gamma, \mathbf{r}) = P_{n_3}^{|k-\lambda|}(\cos\theta)\exp[i(k-\lambda)\chi_v]\phi_e \times \exp(i\lambda\phi)\, d_{0k}^J(\beta)\exp(-ik\gamma), \quad (7)$$

where $\Phi_e^\lambda = \phi_e \exp(i\lambda\phi)$, $D_{0k}^J(\beta, \gamma) = d_{0k}^J(\beta)\exp(-ik\gamma)$ and χ_v is the angle which represents the rotation of the vibrational angular momentum. Hence, we may obtain the symmetries of $\Psi_{V_3}^{J,k,\lambda}$ by considering the individual symmetries of the vibrational functions (spherical harmonics) $P_{n_3}^{|l|}(\cos\theta)\exp(il\chi_v)$, the electronic functions $\phi_e \exp(i\lambda\phi)$ and the rotational functions $d_{0k}^J(\beta)\exp(-ik\gamma)$. This is done in table 1, where the usual notation $l = k - \lambda$ is introduced, and the notations

$$\phi_{V_3}^l(\theta) = P_{n_3}^{|l|}(\cos\theta)\exp(il\chi_v), \quad (8)$$

$$\Phi_{V_3}^{k,\lambda}(\theta, \mathbf{r}) = \phi_{V_3}^l(\theta)\,.\,\phi_e \exp(i\lambda\phi), \quad (9)$$

are used for the vibrational and vibronic functions.

From table 1 (a), it can be seen that $k = 0$ vibronic functions arise from vibrational states with $l = \pm 1$; $k = \pm 1$ functions from states with $l = 0, \pm 2$ etc. Denoting the electronic wavefunctions with $\lambda = \pm 1$ by $\Phi_e^\pm$, functions which

form a basis for the symmetry-adapted ro-vibronic wavefunctions in table 1 (*b*) can thus be written as follows,

$$\left.\begin{array}{lll} k=0, \quad \lambda=\pm 1, & \Phi_{V_3}{}^{J,k,\lambda}=P_{n_3}{}^{|1|}\,\Phi_e{}^{\pm}\,D_{00}{}^{J} & (\Sigma_g{}^{+},\,\Sigma_g{}^{-}), \\ k=\pm 1, \quad \lambda=\pm 1, & \Phi_{V_3}{}^{J,k,\lambda}=P_{n_3}{}^{|0|}\,\Phi_e{}^{\pm}\,D_{0\pm 1}{}^{J} & \\ k=\pm 1, \quad \lambda=\mp 1, & \Phi_{V_3}{}^{J,k,\lambda}=P_{n_3}{}^{|2|}\,\Phi_e{}^{\mp}\,D_{0\pm 1}{}^{J} & (\Sigma_u{}^{+},\,\Sigma_u{}^{-}), \\ k=\pm 2, \quad \lambda=\pm 1, & \Phi_{V_3}{}^{J,k,\lambda}=P_{n_3}{}^{|1|}\,\Phi_e{}^{\pm}\,D_{0\pm 2}{}^{J} & \\ k=\pm 2, \quad \lambda=\mp 1, & \Phi_{V_3}{}^{J,k,\lambda}=P_{n_3}{}^{|3|}\,\Phi_e{}^{\mp}\,D_{0\pm 2}{}^{J} & (\Sigma_g{}^{+},\,\Sigma_g{}^{-}). \end{array}\right\} \tag{10}$$

The individual wavefunctions (10) are not themselves irreducible representations of the $D_{\infty h}$ point group. Symmetry-adapted functions can only be obtained by taking the following combinations of $\Phi_e{}^{\pm}$ and $D_{0\pm k}{}^{J}$:

$$\left.\begin{aligned} D_{0,k}{}^{J}(+)&=\frac{1}{\sqrt{2}}\,(D_{0k}{}^{J}+D_{0-k}{}^{J}), \\ D_{0,k}{}^{J}(-)&=\frac{1}{\sqrt{2}}\,(D_{0k}{}^{J}-D_{0-k}{}^{J}), \\ X&=\frac{1}{\sqrt{2}}\,(\Phi_e{}^{+}+\Phi_e{}^{-}), \\ Y&=-\frac{i}{\sqrt{2}}\,(\Phi_e{}^{+}-\Phi_e{}^{-}). \end{aligned}\right\} \tag{11}$$

The symmetries of the component basis functions may now be summarized as follows :

(i) $D_{00}{}^{J}$ has symmetry $\Sigma_g{}^{+}$ if J is even, $\Sigma_g{}^{-}$ if J is odd. $D_{0k}{}^{J}(+)$ has symmetry $\Sigma_g{}^{+}$ if J is even, $\Sigma_g{}^{-}$ if J is odd, these symmetries being interchanged for $D_{0k}{}^{J}(-)$.

(ii) X has symmetry $\Sigma_u{}^{+}$, Y has symmetry $\Sigma_u{}^{-}$. X, Y are the two components of a linear $^2\Pi_u$ state ; they correspond to the $\tilde{X}\,^2A_1$ and $\tilde{A}\,^2B_1$ states of $CH_2{}^{+}$ respectively.

(iii) $P_V{}^{|l|}$ has symmetry $\Sigma_g{}^{+}$ if l is even, $\Sigma_u{}^{+}$ if l is odd.

The bond stretching expansion functions $\Phi_{V_1}(R_1)$ and $\Phi_{V_2}(R_2)$ are expressed in terms of Morse Oscillator basis functions, described fully earlier [3]. Symmetry adapted products of these may be formed

$$\left.\begin{aligned} \text{(iv)}\ \Phi_{V_1,V_2}(\Sigma_g{}^{+})&=\frac{1}{\sqrt{2}}\,(\Phi_{V_1}(R_1)\Phi_{V_2}(R_2)+\Phi_{V_1}(R_2)\Phi_{V_2}(R_1)), \\ \Phi_{V_1,V_2}(\Sigma_u{}^{+})&=\frac{1}{\sqrt{2}}\,(\Phi_{V_1}(R_1)\Phi_{V_2}(R_2)-\Phi_{V_1}(R_2)\Phi_{V_2}(R_1)). \end{aligned}\right\} \tag{12}$$

The full set of symmetry adapted expansion functions may now be obtained by combining these bond stretching functions with $\Phi_{V_3}{}^{J,k,\lambda}(\theta,\,\beta,\,\gamma)$. This is

Table 1. Symmetries of vibronic (8) and ro-vibronic (9) expansion functions in $D_{\infty h}$.

(*a*) Vibronic wavefunctions $\Phi_V{}^{k,\lambda}(\theta)$.

$\phi_V{}^l(\theta)$		$\phi_e \exp(i\lambda\phi)$		$\Phi_V{}^{k,\lambda}(\theta, \mathbf{r})$	
l	Symmetry	λ	Symmetry	$k=l+\lambda$	Symmetry
0	Σ_g^+	±1	Π_u	±1	Π_u
±1	Π_u			0, ±2	Σ_g^+, Σ_g^-, Δ_g
±2	Δ_g			±1, ±3	Π_u, Φ_u
±3	Φ_u			±2, ±4	Δ_g, Γ_g

(*b*) Ro-vibronic wavefunctions $\Phi_V{}^{J,k,\lambda}(\theta, \beta, \gamma, \mathbf{r})$.

$\Phi_V{}^{k,\lambda}(\theta, \mathbf{r})$		$d_{0k}{}^J(\beta) \exp(-ik\gamma)$	$\Phi_V{}^{J,k,\lambda}(\theta, \beta, \gamma, \mathbf{r})$
k	Symmetry	Symmetry	Symmetry
0	Σ_g^+	Σ_g^+ (J even) Σ_g^- (J odd)	Σ_g^+ (J even) Σ_g^- (J odd)
0	Σ_g^-	Σ_g^+ (J even) Σ_g^- (J odd)	Σ_g^- (J even) Σ_g^+ (J odd)
±1	Π_u	Π_g	Σ_u^+, Σ_u^-
±2	Δ_g	Δ_g	Σ_g^+, Σ_g^-

facilitated by first forming the following combinations of the ro-vibronic functions given in (10):

$$\Phi_{V_3}{}^{J,k,\lambda}(\pm) = \frac{i^{|k|}}{\sqrt{2}} (\Phi_{V_3}{}^{J,k,\lambda}(\theta, \beta, \gamma) \pm \Phi_{V_3}{}^{J,-k,-\lambda}(\theta, \beta, \gamma)) \tag{13}$$

and then using prescriptions (11). The factor $i^{|k|}$ is introduced in (13) to give a real hamiltonian matrix, as was found necessary in [1].

The complete set of symmetry adapted ro-vibronic expansion functions are listed in table 2, for $J=0$, 1, 2, and apply to any $^2\Pi_u$ Renner–Teller molecule. We will refer to these expansion functions by (V_1, V_2, V_3), where V_1, V_2, V_3 are integers which define the expansion functions for R_1, R_2 and θ respectively. For molecules which do not possess high symmetry (i.e. have $C_{\infty V}$ symmetry when linear), the correct symmetry-adapted ro-vibronic functions will be obtained by merely dropping the 'g' and 'u' from those given in table 2. For molecules which have 'g' symmetry when linear (e.g. the linear $^1\Delta_g$ state of O_3) merely interchange 'g' and 'u' in table 2.

Table 2. Ro-vibronic expansion functions for CH_2^+, for $J=0, 1, 2$, classified in $D_{\infty h}$ symmetry. Only the functions for one symmetry species are given explictly. Those for the remaining symmetries are obtained by carrying out permutations on the first set of functions. These permutations are given in the table.

Symmetry in $D_{\infty h}$			Expansion function
$J=0$	$J=1$	$J=2$	
Σ_g^+			$k=0$: $\Phi_{V_1,V_2}(\Sigma_g^+)P_n^{\|1\|}\, XD_{00}{}^J$
	Σ_g^-		$k=\pm 1$: $\frac{1}{\sqrt{2}}\Phi_{V_1,V_2}(\Sigma_u^+)P_n^{\|0\|}[iXD_{01}{}^J(+)-YD_{01}{}^J(-)]$ and $\frac{1}{\sqrt{2}}\Phi_{V_1,V_2}(\Sigma_u^+)P_n^{\|2\|}[iXD_{01}{}^J(+)+YD_{01}{}^J(-)]$
		Σ_g^+	$k=\pm 2$: $\frac{1}{\sqrt{2}}\Phi_{V_1,V_2}(\Sigma_g^+)P_n^{\|1\|}[XD_{02}{}^J(+)+iYD_{02}{}^J(-)]$ and $\frac{1}{\sqrt{2}}\Phi_{V_1,V_2}(\Sigma_g^+)P_n^{\|3\|}[XD_{02}{}^J(+)-iYD_{02}{}^J(-)]$
Σ_u^+	Σ_u^-	Σ_u^+	Interchange $\Phi_{V_1,V_2}(\Sigma_g^+)$ and $\Phi_{V_1,V_2}(\Sigma_u^+)$
Σ_g^-	Σ_g^+	Σ_g^-	Interchange X and iY
Σ_u^-	Σ_u^+	Σ_u^-	Interchange $\Phi_{V_1,V_2}(\Sigma_g^+)$ and $\Phi_{V_1,V_2}(\Sigma_u^+)$; Interchange X and iY

3. The implementation of the variational method

Now that the form of the hamiltonian H and the expansion functions Φ have been described, it only remains to discuss the evaluation of the matrix elements $\langle\Phi_r|H|\Phi_s\rangle$. Following our earlier work [1, 3], the integrations over R_1, R_2, θ are performed numerically using Gauss quadrature, and the matrix elements of $\hat{\mathbf{\Pi}}$ can be evaluated analytically.

Because the dominant Renner–Teller effect is given by the $(\hat{\Pi}_z+\hat{L}_z)^2$ operator in H_{VR}, it was decided not to include $\hat{\mathbf{L}}$ in the other parts of H_{VR}. Furthermore it was also decided to replace the electronic integrals by their values in $D_{\infty h}$ symmetry viz.

$$\left.\begin{aligned}&\langle X|\hat{L}_z{}^2|X\rangle=\hbar^2=\langle Y|\hat{L}_z{}^2|Y\rangle,\\&\langle X|\hat{L}_z|Y\rangle=-i\hbar.\end{aligned}\right\}\tag{14}$$

The reason for doing this is that Peric, Buenker and Peyerimhoff [14] have examined the effects of replacing (14) by

$$\left.\begin{aligned}&\langle X|\hat{L}_z|Y\rangle=-i\hbar B(\theta),\\&\langle X|\hat{L}_z{}^2|X\rangle=\hbar^2\, C^{11}(\theta),\quad \langle Y|\hat{L}_z{}^2|Y\rangle=\hbar^2\, C^{22}(\theta),\end{aligned}\right\}\tag{15}$$

in their Renner–Teller investigations on bending vibrations in NH_2. From *ab initio* calculation, they evaluated B, C^{11} and C^{22} over a wide range of C_{2v} geometries, to find that the important parameter $B(\theta)$ was almost constant, whereas $C^{11}(\theta)$ and $C^{22}(\theta)$ varied between 1·0 and 2·5. They found that the effects of including these variations in their calculations were very slight ; $B(\theta)$ affected levels by a wavenumber or very much less and $C^{11}(\theta)$, $C^{22}(\theta)$ shifted the levels by a nearly constant amount of 17 cm^{-1} for the $\tilde{X}$ state and 14 cm^{-1} for the $\tilde{A}$ state. This latter effect is like a diagonal Born–Oppenheimer correction, and will be almost negligible compared to errors in the form of the potential energy surfaces discussed in the next section.

At this stage it is appropriate to outline the differences between our approach and the earlier work of Jungen and Merer (JM) [12], Dixon, Duxbury and co-workers (DD) [11], and Buenker, Peyerimhoff and co-workers (BP) [14].

All start from hamiltonians which can be derived from the large amplitude bending vibrational hamiltonian $H_b(\theta)$ of Hougen, Bunker and Johns [4]. (JM) and (BP) use the semi-rigid-bender form [17] of this hamiltonian, where the change of bond length with angle is included in the form of the kinetic energy ; (DD) take account of this in a different way. The full hamiltonian used by these workers may be expressed

$$H = H_b(\theta) + A(\theta)(\hat{\Pi}_z + \hat{L}_z)^2 + V(\theta), \tag{16}$$

where

$$H_b(\theta) = a_1(\theta)\frac{\partial^2}{\partial\theta^2} + a_2(\theta)\frac{\partial}{\partial\theta} + a_3(\theta). \tag{17}$$

Variational calculations are performed using this hamiltonian, for the bending ro-vibrational energy levels. Expansion functions of the form

$$\Psi^{v,\lambda,k}(\theta, \phi, \gamma) = \psi_v{}^l(\theta)\Phi_e{}^\lambda(\phi)\exp(ik\gamma) \tag{18}$$

are used, which it will be noticed is similar to the form of (6). The remaining differences between the theoretical aspects of the three authors need not concern us ; all demonstrate that they reproduce each others results using the same potentials. In passing we note that (JM) find it an advantage to use a basis set which is correct in the linear limit, for the same reasons as we discussed in § 2. (BP) find that they can proceed using any value of l (i.e. not $l = k - \lambda$), provided they look after the singular terms in a special way. (DD) on the other hand use what is called the ' bent molecule approach ' where the off diagonal matrix element contains the $\hat{\Pi}_z\hat{L}_z$ operator.

Because we are not interested in least squares fit procedures for the identification of spectra, and it is possible to label our states from the energies we obtain, we have not undertaken any transformation of the matrix to facilitate labelling. It will indeed be observed that our bending expansion functions show very substantial mixing due to the electrostatic splitting from the difference in the potentials in the off diagonal position. But we do include sufficient expansion functions to guarantee convergence.

The major improvement in our work is that we include the effects of stretching motions by including the R_1, R_2 variables in the hamiltonian. Although the other authors take account of the variation of bond length with bond angle, it is not possible for them to pick up Fermi resonance effects, whereas our method obtains this automatically. Fermi resonance effects in our method can be observed from an examination of the eigenvectors.

The only good quantum number in our calculation is J (and M), whereas the other authors must assume that k is a good quantum number, and indeed they find vibrational levels corresponding to the hypothetical $J=0$ levels for each k value.

Our theory will therefore be able to observe any new effects in this problem due to Fermi resonance, and also for each J value, will determine all the rotational levels, e.g. if $J=1$, it will obtain levels usually labelled $k=0$ and $k=\pm 1$. Unfortunately it is not possible to make a *direct* comparison between our work and these other approaches, because we need full-3-dimensional potential energy surfaces $V(R_1, R_2, \theta)$. However some comparison may be obtained from our calculations if no excited stretching vibrational expansion functions are included in the variational calculation; these results will produce a bending vibrational spectrum.

4. Analytical potential functions for $CH_2^+(^2\Pi_u;\ \tilde{X}\,^2A_1, \tilde{A}\,^2B_1)$

Potential functions for the $\tilde{X}\,^2A_1$ and $\tilde{A}\,^2B_1$ components of the degenerate $^2\Pi_u$ pair of states for CH_2^+ are constructed by the method outlined elsewhere [18]. In the present work, we are only interested in regions of the potentials close to the equilibrium ground state configuration, as a means of investigating the ro-vibronic variation procedure introduced in § 2. We are not at this stage interested in reproducing all of the topological phenomena (conical intersections) on which complete potentials must be based. Our potentials will however be valid for linear (degenerate) regions close to equilibrium, and we will therefore impose the correct angular dependence for small displacements from linearity [18].

In assessing the value of the potentials for further dynamical studies, it is instructive to consider the asymptotic behaviour of the true surfaces (that include conical intersections) along $C_{\infty v}$ and C_{2v} dissociation channels. There are two sets of dissociation channels associated with CH_2^+ states of $^2\Pi_u$ and $^2\Sigma_g^+$ symmetries in $D_{\infty h}$. These are

$$HCH^+(^2\Pi_u)\rightarrow\begin{cases}C^+(^2P_u)+H_2(\tilde{X}\,^3\Sigma_g^+)\\ H(^2S_g)+CH^+(\tilde{a}\,^3\Pi)\end{cases} \tag{19}$$

and

$$HCH^+(^2\Sigma_g^+)\rightarrow\begin{cases}C^+(^2P_u)+H_2(\tilde{a}\,^1\Sigma_u^+)\\ H(^2S_g)+CH^+(\tilde{X}\,^1\Sigma^+).\end{cases} \tag{20}$$

These dissociation schemes can be written down immediately on inspection of the correlation rules for $C_{\infty v}$ extractions of an H atom and C_{2v} extractions of a C^+ ion [7] (we note, in passing that there will be a further $^2\Sigma_g^+$ channel leading to $C^+(^2P_u)+H_2(\tilde{A}\,^1\Sigma_u^+)$ for short H–H separations, which will lead to complications in deriving a full ^2A potential).

Comparing (19) and (20), we can see that there will be surface intersections along $C_{\infty v}$ dissociation channels, since the linear $D_{\infty h}$ ground state had $^2\Pi_u$ symmetry, but the asymptotic $H+CH^+$ dissociation fragments will correspond to a state with $^2\Sigma^+$ symmetry in $C_{\infty v}$. Following the arguments given in [18], a full CH_2^+ potential with $^2A'$ symmetry in C_s must therefore be constructed as the eigenvalue of a 2×2 matrix whose diagonal potentials dissociate according to

(19) and (20) respectively. A full $^2A''$ potential is, however, single valued, dissociating everywhere according to (19) (the $^2\Pi_u$ state has two components, of $^2A'$ and $^2A''$ symmetry).

If we neglect the occurrences of surface intersections however, then an adiabatic ground $^2A'$ state of CH_2^+ would dissociate according to the following scheme :

$$CH_2^+(^2A') \rightarrow \begin{cases} C^+(^2P_u) + H_2(\tilde{X}\,^1\Sigma_g^+) \\ H(^2S_g) + CH(\tilde{X}\,^1\Sigma^+). \end{cases} \tag{21}$$

In an earlier work [19] a ground state potential for $CH_2^+(^2A')$, based on (21), was constructed using *ab initio* data of Bartholomae *et al.* [20]. It is therefore expected that this potential is valid for all regions of space except those close to linear structures where intersections occur, and should therefore be useful for many dynamical studies. In deriving a corresponding excited $^2A''$ state potential, which is valid in regions close to equilibrium and is degenerate with $^2A'$ in linear configurations, it is sufficient to write the excited state potential as

$$V(^2A'') = V(^2A') + \sin^n\theta \,.\, V^{(3)}, \tag{22}$$

where θ is the bond angle and $n = |\Lambda' - \Lambda''| = 2$ gives the correct relative angular dependence of the A' and A'' components of a Π state close to linearity [18]. $V^{(3)}$ is a three-body term defined by

$$V^{(3)} = \prod_{i=1}^{3} [1 - \tanh(\gamma_i \rho_i/2)] V_0 \left[\left(1 + \sum_i c_i \rho_i + \sum_{i \leqslant j} c_{ij} \rho_i \rho_j \right) \right], \tag{23}$$

where $\rho = R_i - R_i^0$ are bond displacement coordinates, and R_i^0, γ_i, V_0 and c_i, c_{ij} are parameters to be determined from $CH_2^+(^2A'')$ data. Comparing (19), (20) and (21), it can be seen that a $^2A''$ potential constructed on these lines will be valid in the $C^+ + H_2$ channel, but not in the $H + CH^+$ channel, and will therefore be of little use for dynamical studies involving inelastic collisions.

Our current interests, however, are only in the low-lying ro-vibronic levels of the $^2A'$ and $^2A''$ states, and we have therefore constructed a $^2A''$ potential for CH_2^+ by carrying out a least squares fit of the parameters in (23) to a set of *ab initio* data.

There have been a number of recent *ab initio* studies of the $^2A''$ state of CH_2^+ [21–23]; however, these have been concerned primarily with C_{2v} approaches of C^+ to H_2, and not with regions nearer linearity. In the present work, spin-unrestricted SCF calculations have been carried out using a modified version [24] of the HONDO system of programs [25]. The basis set employed is the Dunning [26] double-zeta contraction of the primitive set of Huzinaga [27], supplemented by a set of *d* functions (exponent 0·75) on C and a set of *p* functions (exponent 1·0) on H. Energies were calculated at the same forty-nine points used in [20] (see table 1). At this level of theory, the global minimum in the $^2A''$ surface (corresponding to a linear geometry) has a total energy of $-38{\cdot}56993$ hartrees and a C–H bond length of 1·083 Å. For comparison, CEPA calculations with a large basis set extrapolate to give a C–H length of 1·092 Å at the minimum [20].

Since the *ab initio* data of Bartholomae *et al.* [20] were obtained from configuration interaction calculations, the new data have been scaled to the $^2A'$ potential [19] before being used in the least squares procedure. This was carried out as follows. A comparison was made between the geometries of the (linear) equilibrium $^2A''$ state as calculated above, and the linear saddle point of the $^2A'$ potential, as obtained by differentiation of the potential in [19]. All *ab initio* $^2A''$ bond lengths were then scaled linearly such that the geometries of these two stationary points were identical. Similarly, the energy of the calculated $^2A''$ minimum was equated to that of the $^2A'$ saddle point, all remaining *ab initio* energies then taken relative to this. The $CH_2^+(\tilde{A}\ ^2A'')$ potential was then derived from the scaled *ab initio* data, and the parameters are given in table 3.

Table 3. Potential energy functions for $CH_2^+(\tilde{X}\ ^2A_1)$ and $CH_2^+(\tilde{A}\ ^2\Pi_u\ ;\ ^2B_1)$.

(*a*) Diatomic potentials.

	a_1/Å^{-1}	a_2/Å^{-2}	a_3/Å^{-3}	D_e/eV	R_e/Å
$CH^+(\tilde{X}^1\Sigma^+)$	2·4558	0·0000	0·0000	4·2548	1·1309
$H_2(\tilde{X}^1\Sigma_g^+)$	3·8795	3·7409	3·2546	4·7501	0·7417

$$V_{AB}^{(2)}(R) = -D_e(1 + a_1\rho + a_2\rho^2 + a_3\rho^3)\exp(-a_1\rho)$$

$$\rho = R - R_e$$

(*b*) Triatomic potentials.

	$V_X^{(3)}$	$V_A^{(3)}$
$C_1 = C_2$/Å^{-1}	2·1122	0·8912
C_3	0·2400	−0·2684
$C_{11} = C_{22}$/Å^{-2}	−34·2341	0·4647
C_{33}	−20·1652	−0·0661
C_{12}	−37·8638	0·4252
$C_{13} = C_{23}$	40·1598	0·0293
V_1^0/eV	−0·1691	0·4888
$\gamma_1 = \gamma_2$/Å^{-1}	2·5484	3·7667
γ_3	4·4975	3·4790
$R_1^0 = R_2^0$/Å	1·1124	1·7220
R_3^0	2·2220	3·4355

$R_1 = R(\mathrm{CH})$, $R_2 = R(\mathrm{CH}')$, $R_3 = R(\mathrm{HH}')$

$$V^{(3)}(R_1, R_2, R_3) = \left[\prod_{i=1}^{3}(1 - \tanh[\gamma_i\rho_i/2])\right] V_1^0\left(1 + \sum_i c_i\rho_i + \sum_{i\leqslant j} c_{ij}\rho_i\rho_j\right)$$

$$\rho_i = R_i - R_i^0$$

$$V_{CH_2^+}(\tilde{X}\ ^2A_1) = \sum_{i=1}^{3} V^{(2)}(R_i) + V_X^{(3)}$$

$$V_{CH_2^+}(\tilde{A}\ ^2\Pi_u, {}^2B_1) = V_{CH_2^+}(\tilde{X}\ ^2A_1) + \sin^2(\theta)\ .\ V_A^{(3)}$$

$$\theta = \widehat{\mathrm{HCH}}$$

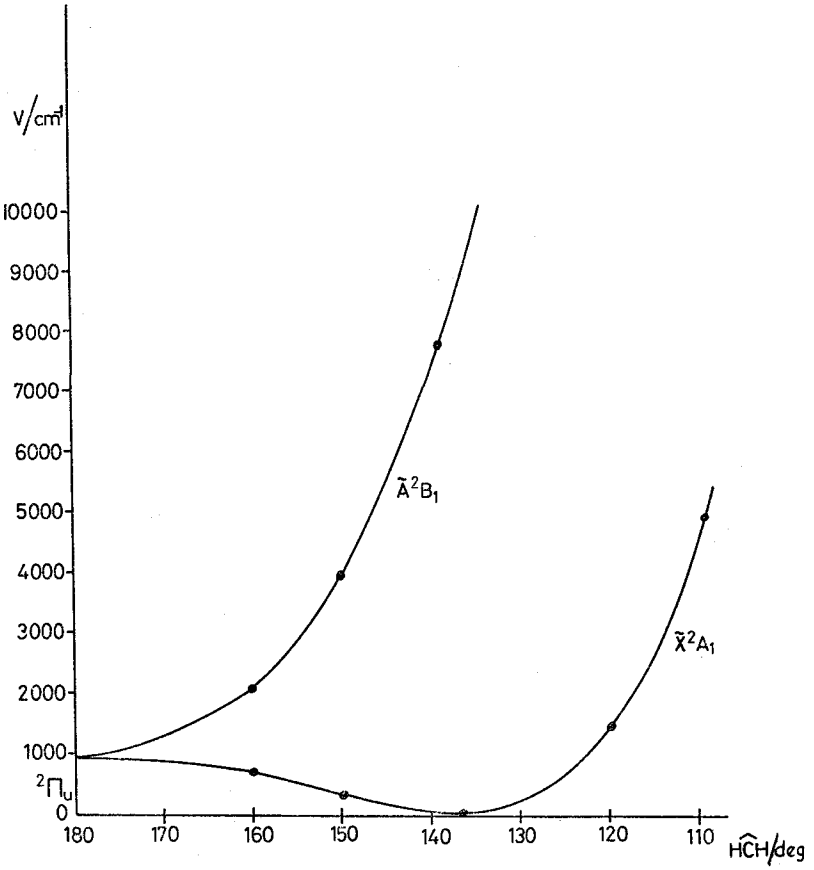

Diagrammatic representation of the optimized bending potentials of $CH_2^+(\tilde{X}\,^2A_1)$ and $CH_2^+(\tilde{A}\,^2B_1)$.

In the figure, the C_{2v} minimum energy paths are plotted for these two $^2A'$ and $^2A''$ surfaces. It will be seen that the bending frequencies will be very different for the two states, the $^2A'$ being quasi-linear and the $^2A''$ being strongly linear.

We may also comment on the probable accuracy of these '*ab initio*' surfaces, based on our experience on the use of *ab initio* data for the determination of frequencies of H_2O [28]. The $^2A'$ state, being determined with CI wavefunctions, we anticipate to yield frequencies which are of the order of 50 cm^{-1} too high for the fundamentals. The $^2A''$, determined by the UHF method will certainly have a greater error for the stretching frequencies, perhaps as much as 150 cm^{-1}, and probably have a greater error for the bending motion, perhaps 100 cm^{-1}. These remarks should be born in mind comparing the results in the next section with any forthcoming experimental frequencies, especially for the higher energies, where the errors will be much greater.

5. The ro-vibronic energy levels of CH_2^+

The crucial factor in these calculations is to have sufficient bending vibration expansion functions $P_n^{|l|}(\cos\theta)$ such that the bending vibrations of both the

states are adequately represented as well as their strong interaction. Initial calculations were therefore performed to find optimum combinations of the $P_n^{|l|}$ which could then be included in the full calculations involving both stretching and bending expansion functions.

For example for the $J=1$, Σ_g^- and Σ_u^- states, optimum combinations were found by using expansion functions $\Phi_{00}(\Sigma_g^+)P_n^{|1|}\,XD_{00}{}^J$, $n=1, 2, \ldots, N$, with the hamiltonian

$$H_V+\frac{1}{8\cos^2\theta/2}\left(\frac{1}{\mu R_1{}^2}+\frac{1}{\mu R_2{}^2}+\frac{2\cos\theta}{mR_1R_2}\right)[\hat{\Pi}_z+\hat{L}_z]^2. \tag{24}$$

In this way coefficients a_{Vs} for the optimized combinations

$$\Phi_V{}^1(\theta)=\sum_{s=1}^{N} a_{Vs}P_s^{|1|}(\cos\theta), \tag{25}$$

are obtained which are then used as orthonormal expansion functions in the full calculations.

This was even more important for the $P_n^{|0|}(\cos\theta)$ and $P_n^{|2|}(\cos\theta)$ combinations. These were obtained using the same Hamiltonian (24), and the expansion set

$$\begin{cases}\dfrac{1}{\sqrt{2}}\,\Phi_{00}(\Sigma_g^+)P_n{}^0[iXD_{01}{}^J(+)-YD_{01}{}^J(-)]\\[2ex]\dfrac{1}{\sqrt{2}}\,\Phi_{00}(\Sigma_g^+)P_n{}^2[iXD_{01}{}^J(+)+YD_{01}{}^J(-)].\end{cases} \tag{26}$$

Diagonalization of this matrix yields expansion functions

$$\Phi_V{}^{0,2}(\theta)=\sum_{s=1}^{N}(i(b_{Vs}P_s{}^0+c_{Vs}P_s{}^2)XD_{01}{}^J(+)+(b_{Vs}P_s{}^2-c_{Vs}P_s{}^0)YD_{01}{}^J(-)) \tag{27}$$

which are then ready for use in the full calculations.

The coefficients a_{Vs}, b_{Vs}, c_{Vs} from these calculations have no apparent features, and the bending labels and attachment to the lower or upper state can only be obtained from an examination of the eigenvalues. Note that these initial calculations include the key Renner–Teller interaction $\hat{L}_z\hat{\Pi}_z$ and the electrostatic splitting effects. In the full calculations, $\Phi_V{}^1(\theta)$ and $\Phi_V{}^{0,2}(\theta)$ interact through terms such as $\hat{\Pi}_x\hat{\Pi}_z$ in H_{VR}. The basis functions such as $\Phi_V{}^1(\theta)$, $\Phi_V{}^{0,2}(\theta)$, will represent the bending parts of the general expansion functions (V_1, V_2, V_3) for the full calculations†. Following our usual convention, sufficient expansion functions are included for convergence, and are given by the parameters $V_1\leqslant N_1$, $V_2\leqslant N_2$, $V_3\leqslant N_3$ with M_1, M_2, M_3 denoting the number of integration points required to evaluate the matrix elements. The number of bending functions used in the initial calculations with the Hamiltonian (24) is denoted by $N_3{}^{\max}$.

† Do not confuse the expansion set (V_1, V_2, V_3) with the assignments $(v_1v_2{}^k v_3)$ in table 5. The expansion set refer to the coordinates R_1, R_2, θ respectively whilst the assignments refer to symmetric stretch, bend, asymmetric stretch, by convention.

Table 4. Ro-vibronic band origins of CH_2^+, in cm^{-1}, measured relative to the $(000]_{J,k=0}$ energy level of the $\tilde{X}\,^2A_1$ state. The table predicts pure bending frequencies arising from an analysis of a $(00V_3)$ basis set (see text). The energy levels of the $\tilde{X}\,^2A_1$ state are written n_k, where n denotes the bending quantum number for a bent molecule. Those for the $\tilde{A}\,^2B_1(^2\Pi_u)$ state are written v^k, where v denotes the linear angle bending quantum number, k is the z-component of the total angular momentum in both cases ($|k| \leqslant J$). The numbers in parentheses are the $k=1$ ($J=1$) energy levels, calculated without the term $2\hat{\Pi}_z\hat{L}_z$ in the ro-vibronic hamiltonian.

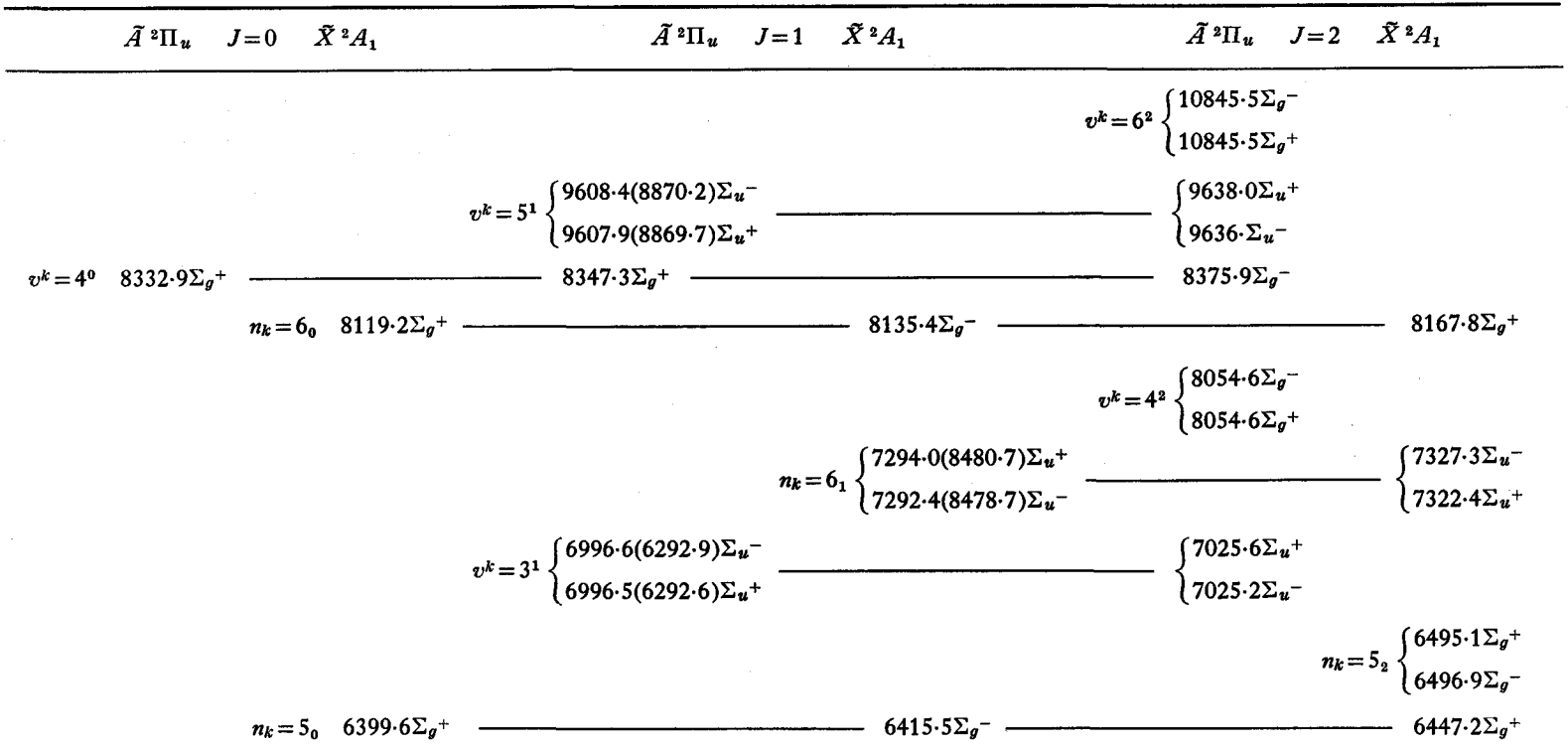

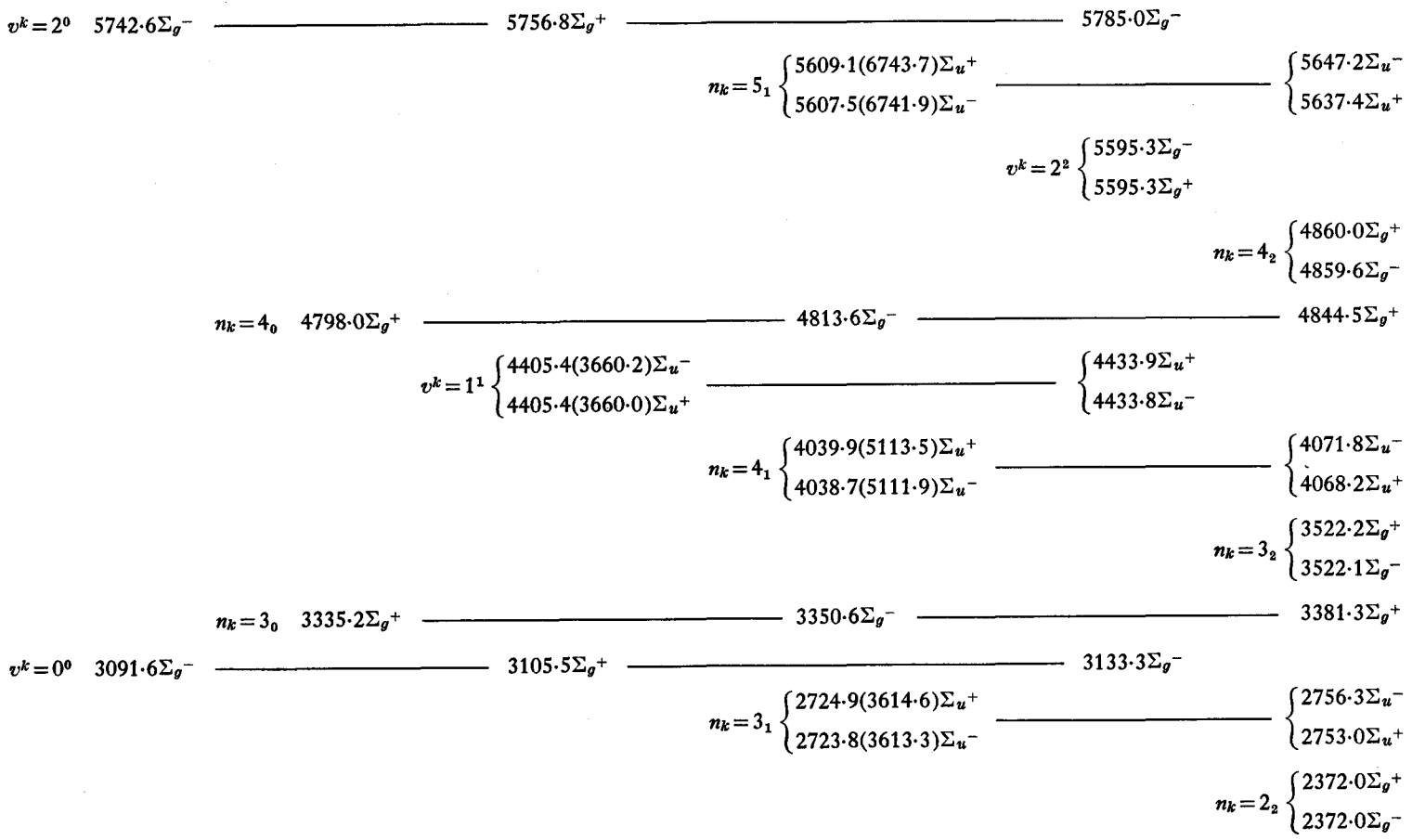
$v^k=2^0$ 5742·6Σ_g^-
5756·8Σ_g^+
5785·0Σ_g^-
$n_k=5_1$ 5609·1(6743·7)Σ_u^+ 5607·5(6741·9)Σ_u^-
5647·2Σ_u^- 5637·4Σ_u^+
$v^k=2^2$ 5595·3Σ_g^- 5595·3Σ_g^+
$n_k=4_2$ 4860·0Σ_g^+ 4859·6Σ_g^-
$n_k=4_0$ 4798·0Σ_g^+
4813·6Σ_g^-
4844·5Σ_g^+
$v^k=1^1$ 4405·4(3660·2)Σ_u^- 4405·4(3660·0)Σ_u^+
4433·9Σ_u^+ 4433·8Σ_u^-
$n_k=4_1$ 4039·9(5113·5)Σ_u^+ 4038·7(5111·9)Σ_u^-
4071·8Σ_u^- 4068·2Σ_u^+
$n_k=3_2$ 3522·2Σ_g^+ 3522·1Σ_g^-
$n_k=3_0$ 3335·2Σ_g^+
3350·6Σ_g^-
3381·3Σ_g^+
$v^k=0^0$ 3091·6Σ_g^-
3105·5Σ_g^+
3133·3Σ_g^-
$n_k=3_1$ 2724·9(3614·6)Σ_u^+ 2723·8(3613·3)Σ_u^-
2756·3Σ_u^- 2753·0Σ_u^+
$n_k=2_2$ 2372·0Σ_g^+ 2372·0Σ_g^-

Table 4 (*continued*)

$\tilde{A}\,^2\Pi_u$ $J=0$ $\tilde{X}\,^2A_1$	$\tilde{A}\,^2\Pi_u$ $J=1$ $\tilde{X}\,^2A_1$	$\tilde{A}\,^2\Pi_u$ $J=2$ $\tilde{X}\,^2A_1$
$n_k=2_0$ $2039{\cdot}9\Sigma_g^+$	$2055{\cdot}0\Sigma_g^-$	$2085{\cdot}2\Sigma_g^+$
	$n_k=2_1$ $\begin{cases}1649{\cdot}0(2273{\cdot}9)\Sigma_u^+\\1648{\cdot}2(2272{\cdot}8)\Sigma_u^-\end{cases}$	$\begin{cases}1679{\cdot}2\Sigma_u^-\\1676{\cdot}9\Sigma_u^+\end{cases}$
		$n_k=1_2$ $\begin{cases}1340{\cdot}6\Sigma_g^+\\1340{\cdot}6\Sigma_g^-\end{cases}$
$n_k=1_0$ $943{\cdot}2\Sigma_g^+$	$958{\cdot}1\Sigma_g^-$	$987{\cdot}9\Sigma_g^+$
	$n_k=1_1$ $\begin{cases}903{\cdot}7(1111{\cdot}2)\Sigma_u^+\\903{\cdot}1(1110{\cdot}3)\Sigma_u^-\end{cases}$	$\begin{cases}933{\cdot}5\Sigma_u^-\\931{\cdot}6\Sigma_u^+\end{cases}$
		$n_k=0_2$ $\begin{cases}297{\cdot}4\Sigma_g^+\\297{\cdot}4\Sigma_g^-\end{cases}$
	$n_k=0_1$ $\begin{cases}74{\cdot}3(92{\cdot}8)\Sigma_u^+\\73{\cdot}4(91{\cdot}9)\Sigma_u^-\end{cases}$	$\begin{cases}105{\cdot}0\Sigma_u^-\\102{\cdot}3\Sigma_u^+\end{cases}$
$n_k=0_0$ $0{\cdot}0\Sigma_g^+$	$14{\cdot}9\Sigma_g^-$	$44{\cdot}6\Sigma_g^+$

The first calculations used only the expansion set $(0, 0, V_3)$, i.e. just the lowest Morse Stretching functions with all bending functions. In these calculations all effects will show, except those due to Fermi resonance, for the bending vibrations, and these should show similar characteristics to the calculations of JM, DD and PB. The results are shown in table 4. In the table, results are labelled according to symmetry and k, even though the latter is not a good quantum number. The values for $J=0$, 1 have converged to less than 1 cm^{-1} accuracy, but those for $J=2$ may have an error of 1 or 2 cm^{-1} for the higher levels. In the calculations, $M_1=M_2=4$ and $M_3=26$ were used for the numerical integration. These were found adequate to integrate exactly functions with $N_1=N_2=0$ and $N_3^{max}=22$. $N_3=9$ was used in the full calculations.

For $k=0$, the $J=0$, 1, 2 levels are in full agreement for both the $\tilde{X}$ and $\tilde{A}$ states. It is noted that the bending frequency for the $\tilde{X}$ state is 943 cm^{-1} and for the $\tilde{A}$ state is 2651 cm^{-1}, which is anticipated from the figure. For $J=0$, the $\tilde{X}$ and $\tilde{A}$ vibrational levels completely separate. Anharmonicity effects show in the increasing gaps between successive levels for the $\tilde{X}$ state.

For $k=1$, the $J=1$ and $J=2$ pairs of levels are in good agreement, with the splitting between pairs greater for $J=2$ than for $J=1$. The relative symmetries of the $k=1$ and $k=2$ near-degenerate pairs are consistent with those predicted from theoretical considerations of the asymmetry of the $\tilde{X}\,^2A_1$ state resulting from a linear $^2\Pi_u$ state. Those for the upper state, on the other hand, are more difficult to predict, since for a linear molecule, these are associated with the l-type doubling brought about by interaction with one level and the asymmetric stretch. In table 4, there are no stretching vibrations involved in the calculations, and it is therefore encouraging to find that the splittings of the $k=1$ and $k=2$ pairs are markedly smaller than those for the $\tilde{X}\,^2A_1$ state.

The effect of the Renner–Teller term $2\hat{\Pi}_z\hat{L}_z$ is noticed from the column of results obtained when this term is omitted from the calculations, where it is seen that the $k=1$ levels all lie above the $k=0$ levels in an expected pattern. The effect of the Renner–Teller term is to reorder these $k=1$ levels with respect to the $k=0$ levels, for the lower state, as first noticed by Jungen, Malm and Merer [29]. Thus we see that only for the lowest $(v_2=0)$ level does the $k=1$ level lie above the $k=0$, and for all the remainder $k=1$ lies below $k=0$ and tends to the $k=1$ (v_2) level lying midway between $k=0$ (v_2) and $k=0$ (v_2-1). It is noticed that the $k=1$ level for $v_2=1$ and $v_2=2$ are beneath $k=0$, demonstrating the enormous Renner–Teller effect. Indeed the $k=1$ $(v_2=3)$ at 2724 cm^{-1} is already lying approximately half way between the $v_2=2$ and $v_2=3$, $k=0$ levels.

The effect of the Renner–Teller term on the upper state $k=1$ levels is also significant. It is seen that the $k=1$ (v_2) levels lie half way between the $k=0$ (v_2 and v_2-1) levels, whereas with no Renner–Teller term, they lie about 550 cm^{-1} above the $k=0$ (v_2) levels.

The $k=2$ $(J=2)$ levels are also given for the X state ; they now all lie above the corresponding $J=0$ levels, and indeed the $J=2$ $(k=2)$ and $J=2$ $(k=0)$ levels ultimately become close. For the upper state the $k=2$ (v_2) levels lie close to the $k=0$ (v_2+1) levels. The relative orderings of the various k-levels for given J are consistent with those predicted from theoretical considerations, and this typical behaviour is shown schematically in [7].

Table 5. Ro-vibronic band origins of CH_2^+, in cm^{-1}, measured relative to the $(000)_{J,k=0}$ energy level of the $\tilde{X}\,^2A_1$ state. The table predicts the bend-stretch spectrum arising from an analysis of a $(V_1V_2V_3)$ basis set (see text). The energy levels of the $\tilde{X}\,^2A_1$ state are written $(v_1n_2v_3)_k$, where n denotes the bending quantum number for a bent molecule. Those for the $\tilde{A}\,^2B_1(^2\Pi_u)$ state are written $(v_1v_2{}^k\,v_3)$, where v_2 denote the linear angle bending quantum number. v_1 denotes the symmetric stretch and v_3 the asymmetric stretch in both case, and k is the z-component of the total angular momentum ($|k| \leqslant J$). Not all band origins appear in the table. Only those $k=1$ and $k=2$ levels corresponding to the appropriate $k=0$ levels are listed, with the exception of (12^20), (05^10) and (06^20) for the $\tilde{A}\,^2\Pi_u$ state.

$\tilde{A}\,^2\Pi_u$ $J=0$	$\tilde{X}\,^2A_1$	$\tilde{A}\,^2\Pi_u$ $J=1$	$\tilde{X}\,^2A_1$	$\tilde{A}\,^2\Pi_u$ $J=2$	$\tilde{X}\,^2A_1$
				(02^21) 8759·8Σ_u^-	
				8759·8Σ_u^+	
(04^00) 8184·5Σ_g^-	———	8198·1Σ_g^+	———	8225·0Σ_g^+	
				(04^20) 7888·7Σ_g^-	
				7888·7Σ_g^+	
		(01^11) 7589·2Σ_g^-	———	7616·9Σ_g^+	
		7589·2Σ_g^+		7616·9Σ_g^-	
		(11^10) 7358·5Σ_u^-	———	7387·0Σ_u^+	
		7358·6Σ_u^+		7387·3Σ_u^-	
		(03^10) 6893·8Σ_u^-	———	6921·6Σ_u^+	
		6893·7Σ_u^+		6921·2Σ_u^-	
				$(101)_2$ 6398·1Σ_u^+	
				6398·1Σ_u^-	
				$(130)_2$ 6355·5Σ_g^+	
				6355·4Σ_g^-	

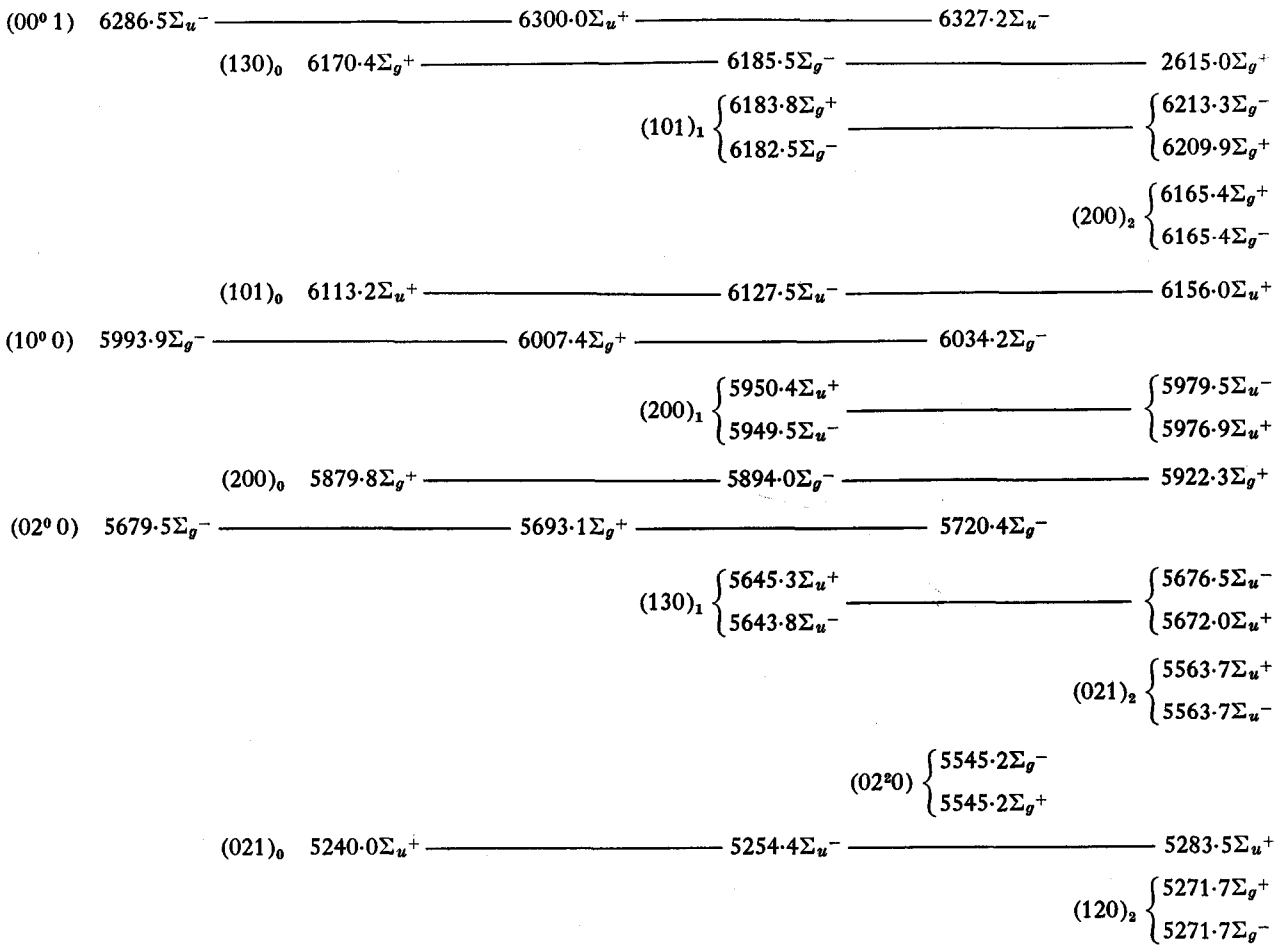
(00⁰1) 6286·5Σu⁻ 6300·0Σu⁺ 6327·2Σu⁻
(130)0 6170·4Σg⁺ 6185·5Σg⁻ 2615·0Σg⁺
(101)1 6183·8Σg⁺ 6182·5Σg⁻ 6213·3Σg⁻ 6209·9Σg⁺
(200)2 6165·4Σg⁺ 6165·4Σg⁻
(101)0 6113·2Σu⁺ 6127·5Σu⁻ 6156·0Σu⁺
(10⁰0) 5993·9Σg⁻ 6007·4Σg⁺ 6034·2Σg⁻
(200)1 5950·4Σu⁺ 5949·5Σu⁻ 5979·5Σu⁻ 5976·9Σu⁺
(200)0 5879·8Σg⁺ 5894·0Σg⁻ 5922·3Σg⁺
(02⁰0) 5679·5Σg⁻ 5693·1Σg⁺ 5720·4Σg⁻
(130)1 5645·3Σu⁺ 5643·8Σu⁻ 5676·5Σu⁻ 5672·0Σu⁺
(021)2 5563·7Σu⁺ 5563·7Σu⁻
(02²0) 5545·2Σg⁻ 5545·2Σg⁺
(021)0 5240·0Σu⁺ 5254·4Σu⁻ 5283·5Σu⁺
(120)2 5271·7Σg⁺ 5271·7Σg⁻

Table 5 (*continued*).

$\tilde{A}\,^2\Pi_u$ $J=0$ $\tilde{X}\,^2A_1$	$\tilde{A}\,^2\Pi_u$ $J=1$ $\tilde{X}\,^2A_1$	$\tilde{A}\,^2\Pi_u$ $J=2$ $\tilde{X}\,^2A_1$
$(120)_0$ $4952{\cdot}8\Sigma_g^+$	$4967{\cdot}2\Sigma_g^-$	$4996{\cdot}0\Sigma_g^+$
	$(021)_1$ $4864{\cdot}5\Sigma_g^+$, $4864{\cdot}5\Sigma_g^-$	$4894{\cdot}7\Sigma_g^-$, $4892{\cdot}6\Sigma_g^+$
		$(040)_2$ $4785{\cdot}5\Sigma_g^+$, $4785{\cdot}3\Sigma_g^-$
$(040)_0$ $4717{\cdot}1\Sigma_g^+$	$4732{\cdot}1\Sigma_g^-$	$4761{\cdot}8\Sigma_g^+$
	$(120)_1$ $4573{\cdot}5\Sigma_u^+$, $4572{\cdot}7\Sigma_u^-$	$4602{\cdot}6\Sigma_u^-$, $4600{\cdot}2\Sigma_u^+$
		$(011)_2$ $4568{\cdot}4\Sigma_u^+$, $4568{\cdot}4\Sigma_u^-$
$(0\,1^1 0)$ $4377{\cdot}6\Sigma_u^-$, $4377{\cdot}5\Sigma_u^+$	$4405{\cdot}2\Sigma_u^+$, $4404{\cdot}9\Sigma_u^-$	
		$(110)_2$ $4283{\cdot}8\Sigma_g^+$, $4283{\cdot}8\Sigma_g^+$
$(011)_0$ $4181{\cdot}7\Sigma_u^+$	$4196{\cdot}2\Sigma_u^-$	$4225{\cdot}1\Sigma_u^+$
	$(011)_1$ $4143{\cdot}8\Sigma_g^+$, $4143{\cdot}1\Sigma_g^-$	$4172{\cdot}8\Sigma_g^-$, $4170{\cdot}8\Sigma_g^+$
	$(040)_1$ $3989{\cdot}6\Sigma_u^+$, $3988{\cdot}2\Sigma_u^-$	$4020{\cdot}3\Sigma_u^-$, $4016{\cdot}2\Sigma_u^+$

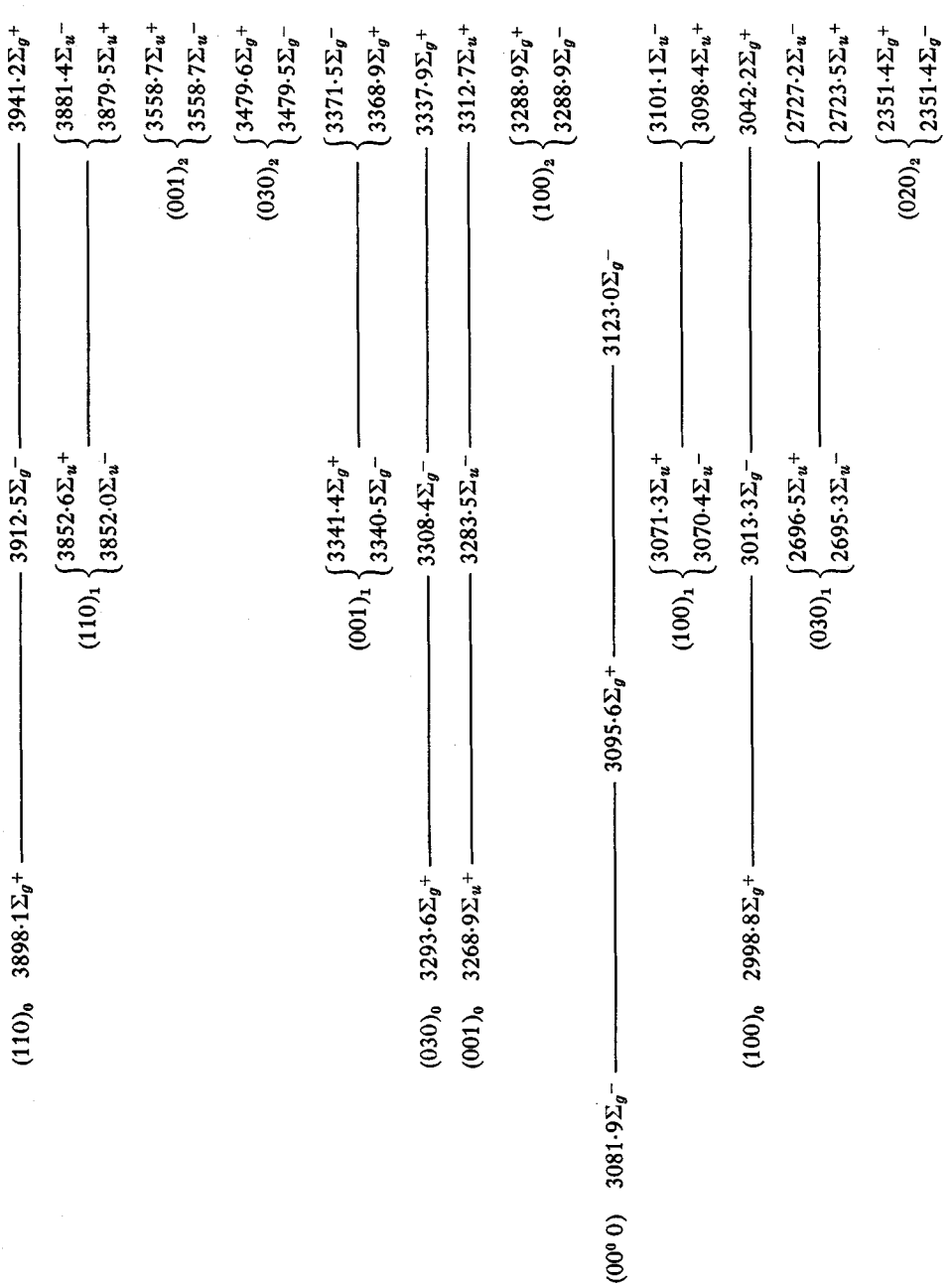
(110)0 3898·1Σg+
3912·5Σg−
3941·2Σg+
(110)1 3852·6Σu+
3852·0Σu−
3881·4Σu−
3879·5Σu+
(001)2 3558·7Σu+
3558·7Σu−
(030)2 3479·6Σg+
3479·5Σg−
(001)1 3341·4Σg+
3340·5Σg−
3371·5Σg−
3368·9Σg+
(030)0 3293·6Σg+
3308·4Σg−
3337·9Σg+
(001)0 3268·9Σu+
3283·5Σu−
3312·7Σu+
(100)2 3288·9Σg+
3288·9Σg−
(00⁰ 0) 3081·9Σg−
3095·6Σg+
3123·0Σg−
(100)1 3071·3Σu+
3070·4Σu−
3101·1Σu−
3098·4Σu+
(100)0 2998·8Σg+
3013·3Σg−
3042·2Σg+
(030)1 2696·5Σu+
2695·3Σu−
2727·2Σu−
2723·5Σu+
(020)2 2351·4Σg+
2351·4Σg−

Table 5 (*continued*)

$\tilde{A}\,^2\Pi_u$	$J=0$	$\tilde{X}^2A_1$	$\tilde{A}\,^2\Pi_u$	$J=1$	$\tilde{X}^2A_1$	$\tilde{A}\,^2\Pi_u$	$J=2$	$\tilde{X}^2A_1$
	$(020)_0$	$2021{\cdot}8\Sigma_g^+$			$2036{\cdot}5\Sigma_g^-$			$2066{\cdot}0\Sigma_g^+$
				$(020)_1$	$1638{\cdot}9\Sigma_u^+$			$1668{\cdot}6\Sigma_u^-$
					$1638{\cdot}1\Sigma_u^-$			$1666{\cdot}2\Sigma_u^+$
							$(010)_2$	$1331{\cdot}9\Sigma_g^+$
								$1331{\cdot}9\Sigma_g^-$
	$(010)_0$	$938{\cdot}1\Sigma_g^+$			$952{\cdot}8\Sigma_g^-$			$982{\cdot}1\Sigma_g^+$
				$(010)_1$	$900{\cdot}4\Sigma_u^+$			$929{\cdot}9\Sigma_u^-$
					$899{\cdot}7\Sigma_u^-$			$927{\cdot}9\Sigma_u^+$
							$(000)_2$	$296{\cdot}0\Sigma_g^+$
								$296{\cdot}0\Sigma_g^-$
				$(000)_1$	$74{\cdot}1\Sigma_u^+$			$104{\cdot}6\Sigma_u^-$
					$73{\cdot}2\Sigma_u^-$			$101{\cdot}9\Sigma_u^+$
	$(000)_0$	$0{\cdot}0\Sigma_g^+$			$14{\cdot}8\Sigma_g^-$			$44{\cdot}4\Sigma_g^+$

The conclusion to be drawn from these results is that the same k pattern is obtained as JM, DD and PB. They of course obtained k levels extrapolated to $J=0$. In this case there has been no difficulty in assigning the various levels to an electronic state, although this may happen for other molecules [12]. From these results there appears no reason to think that significant effects have been omitted in the approximations used by JM, DD and PB.

The results of $J=0, 1, 2$ calculations when stretching expansion functions $v_1>0$, $v_2>0$ are included are given in table 5. For these calculations $N_1=6$, $N_2=6$, $N_3=6$ and $M_1=10$, $M_2=10$, $M_3=26$, with $N_3^{\max}=22$.

The $k=0$, $J=0$ bending levels, with $v_1=v_2=0$ are similar to those in table 4. For the lower state the discrepancy between these is 5, 18, 43, 84, 114 and 208 cm^{-1} and for the upper state 61 and 147 cm^{-1}. These discrepancies represent the slightly different stretching functions which need to be associated with each bending vibration, as well as interaction with other vibrational states.

For comparison purposes only, in table 6 the results for the $\tilde{X}$ state are compared with those from [3], where the ro-vibrational energy levels were determined taking no account of electronic angular momentum. The comparison clearly shows the important effect of the term usually denoted $A\hat{L}_z^2$, and its dependence on vibrational quantum number. Calculations which omit electronic angular momentum are therefore almost valueless, from a predictive point f view.

Table 6. $J=0$ vibronic levels of CH_2^+ (for the $\tilde{X}\,^2\tilde{A}_1$ state), in cm^{-1}, measured relative to the (000) ground state level, determined (*a*) as reported in this work and (*b*) taking no account of orbital angular momentum [3].

Level	(*a*)	(*b*)
021	5240·0	4839·2
120	4952·8	4550·1
040	4717·1	4114·4
011	4181·7	3966·7
110	3898·1	3678·4
030	3293·6	2770·2
001	3268·9	3270·6
100	2998·8	2998·8
020	2021·8	1610·9
010	938·1	718·3
000	0·0	0·0

The stretching fundamentals in the lower state, 2999 cm^{-1} and 3269 cm^{-1} differ from those of the upper state, 2992 cm^{-1} and 3204 cm^{-1}, only slightly. We note at this stage that the expansion functions (26) can only be constructed if we assume identical stretching functions in the X and Y electronic states. For CH_2^+ at least, this factorization is validated by the similarities of the two sets of stretching frequencies. We also observe that the two sequences $(0v_10)_0 \leftarrow (000)_0$ and $(1v_20)_0 \leftarrow (100)_0$ are similar; 938(899), 2022(1954) and 3294(3171). This implies that there are no substantial Fermi-resonances influencing these energy levels.

The assignments of the ro-vibronic energy levels in table 4 and 5 were carried out by inspection of the variational wavefunctions, and selecting the expansion function which corresponds to the largest coefficient in the eigenfunction. Due to our choice of Morse stretching basis functions and the optimized $(0, 0, V_3)$ bending basis functions, the expansion set is very nearly diagonal in the final (V_1, V_2, V_3) analysis, and this method of assignment is generally unambigous. However, care must be taken when isolating the stretching vibrations (20^k0) and (00^k2), for example, both of which have the same symmetries. The symmetry adapted functions in (12) are with respect to *internal* coordinates R_1 and R_2, and not to the *symmetry* coordinates $(1/\sqrt{2})(R_1 \pm R_2)$ for the symmetric and antisymmetric stretches. It follows that the final eigenfunctions will show heavy mixing between the expansion function $[(2, 0, 0)+(0, 2, 0)]$ and $+(1, 1, 0)$ for (20^k0), and $-(1, 1, 0)$ for (00^k2), for example.

Inspection of the wavefunctions in this manner leads to the conclusion that there are no dramatic effects of Fermi-resonance in the tabulated energies, in which any two prominant states interact. However, it can clearly be seen, by comparing the frequencies in table 4 with the corresponding frequencies in table 5, that inclusion of the stretching modes does indeed have a pronounced effect on the resulting energy levels.

Finally, we comment on the convergence of the full variational calculations. The basis $N=6$ $(\Sigma N_i \leqslant N)$ is the maximum basis that we can currently calculate for $k=2$, that gives equal weighting to both of the stretching modes and the bending mode in both electronic states. For consistency therefore all calculations in table 5 were conducted with this basis. For $k=1$, $J=1$, it is however possible to increase the basis to $N=7$, and the results suggest that all wave numbers given in table 5 are converged to a maximum error of 5 cm^{-1}, with the exception of $(130)_1$ and $(03^1 0)$, $(01^1 1)$. The average $N=7$ values for these $(J=1)$ are 5617, 6859 and 7560 cm^{-1}, respectively, which are probably still in error by some 5–10 cm^{-1}. We are currently investigating the possible ways of increasing the scope of our programme to cover large J, which unavoidably leads to large hamiltonian matrices.

6. Conclusion

In this paper we have presented a variational method to determine the ro-vibronic spectra of CH_2^+, a Renner–Teller molecule, for $J=0, 1, 2$, up to about 7000 cm^{-1}. All the expected features of the spectrum appear, including the reordering of the k levels due to the Renner–Teller interaction. Fermi-resonance interactions have been discussed from an examination of the eigenvectors of the matrix. Inaccuracies in the *ab initio* data for the $\tilde{A}$ state mean that there will be considerable errors in the levels associated with that state, as discussed in § 4.

Now that we have established that this method is practicable, we hope to extend it to NH_2, where much other work has already been done. It is more difficult because the height of the barrier to linearity for NH_2 is $\sim 10\,000$ cm^{-1}, thus meaning that there are many more bending levels for the $\tilde{X}$ state below linearity, and this implies that larger matrices have to be diagonalized. But of course there are more effects of Fermi-resonance present, and if it was possible to obtain reasonably accurate potential energy surfaces for both states, then a greater understanding of the observed spectra would be possible.

S.C. acknowledges the support of the SERC over a period of years, which has enabled this research to be carried out. We thank R. H. Nobes for carrying out the *ab initio* calculations reported in § 4. We also acknowledge valuable discussions with I. M. Mills, R. N. Dixon and B. T. Sutcliffe. The set of ro-vibrational programs are available on application to S. Carter.

References

[1] Carter, S., Handy, N. C., and Sutcliffe, B. T., 1983, *Molec. Phys.*, **49**, 745.
[2] Carney, G. D., Sprandel, L. L., and Kern, C. W., 1978, *Adv. chem. Phys.*, **37**, 205.
[3] Carter, S., and Handy, N. C., 1982, *Molec. Phys.*, **47**, 1445.
[4] Hougen, J. T., Bunker, P. R., and Johns, J. W. C., 1970, *J. molec. Spectrosc.*, **34**, 136.
[5] Bunker, P. R., and Stone, J. M. R., 1934, *J. molec. Spectrosc.*, **41**, 310.
[6] Renner, R., 1934, *Z. Phys.*, **92**, 172.
[7] Herzberg, G., 1966, *Electronic Spectra of Polyatomic Molecules* (Van Nostrand).
[8] Pople, J. A., and Longuet-Higgins, H. C., 1958, *Molec. Phys.*, **1**, 372.
[9] Dressler, K., and Ramsey, D. A., 1959, *Phil. Trans. R. Soc.* A, **251**, 553.
[10] Barrow, T., Dixon, R. N., and Duxbury, G., 1974, *Molec. Phys.*, **27**, 1217.
[11] Duxbury, G., and Dixon, R. N., 1981, *Molec. Phys.*, **43**, 255.
[12] Jungen, Ch., and Merer, A. J., 1980, *Molec. Phys.*, **40**, 1 and 25.
[13] Buenker, R. J., Peric, M., Peyerimhoff, S. D., and Marian, R., 1981, *Molec. Phys.*, **43**, 987.
[14] Peric, M., Peyerimhoff, S. D., and Buenker, R. J., 1983, *Molec. Phys.*, **49**, 379.
[15] Sutcliffe, B. T., 1982, *Current Aspects of Quantum Chemistry*, edited by R. Carbo (Elsevier).
[16] Bunker, P. R., and Papousek, D., 1969, *J. molec. Spectrosc.*, **32**, 419.
[17] Bunker, P. R., and Landsberg, B. M., 1977, *J. molec. Spectrosc.*, **67**, 374.
[18] Carter, S., Mills, I. M., and Dixon, R. N., 1984, *J. molec. Spectrosc.* (in the press).
[19] Carter, S., and Handy, N. C., 1982, *J. molec. Spectrosc.*, **95**, 9.
[20] Bartholomae, R., Martin, D., and Sutcliffe, B. T., 1981, *J. molec. Spectrosc.*, **87**, 367.
[21] Liskow, D. H., Bender, C. F., and Schaefer, H. F., 1974, *J. chem. Phys.*, **61**, 2507.
[22] Sakai, S., Kato, S., Morokuma, K., and Kusunoki, I., 1981, *J. chem. Phys.*, **75**, 5398.
[23] Jaquet, R., and Staemmler, V., 1982, *Chem. Phys.*, **68**, 479.
[24] Amos, R. D. (unpublished results).
[25] Dupuis, M., Rys, J., and King, H. F., 1981, *Quant. Chem. Program Exch.*, **13**, 403.
[26] Dunning, T. H., 1970, *J. chem. Phys.*, **53**, 2823.
[27] Huzinaga, S., 1965, *J. chem. Phys.*, **43**, 1293.
[28] Sexton, G. J., and Handy, N. C., 1984, *Molec. Phys.*, **51**, 1321.
[29] Jungen, Ch., Malm, D. N., and Merer, A. J., 1973, *Can. J. Phys.*, **51**, 1471.